

Observation of $\bar{B} \rightarrow D^{(*)} \pi^+ \pi^- \ell^- \bar{\nu}$ Decays in $e^+ e^-$ Collisions at the $\Upsilon(4S)$ Resonance

J. P. Lees,¹ V. Poireau,¹ V. Tisserand,¹ E. Grauges,² A. Palano,^{3a,3b} G. Eigen,⁴ B. Stugu,⁴ D. N. Brown,⁵ L. T. Kerth,⁵ Yu. G. Kolomensky,⁵ M. J. Lee,⁵ G. Lynch,⁵ H. Koch,⁶ T. Schroeder,⁶ C. Hearty,⁷ T. S. Mattison,⁷ J. A. McKenna,⁷ R. Y. So,⁷ A. Khan,⁸ V. E. Blinov,^{9a,9b,9c} A. R. Buzykaev,^{9a} V. P. Druzhinin,^{9a,9b} V. B. Golubev,^{9a,9b} E. A. Kravchenko,^{9a,9b} A. P. Onuchin,^{9a,9b,9c} S. I. Serednyakov,^{9a,9b} Yu. I. Skovpen,^{9a,9b} E. P. Solodov,^{9a,9b} K. Yu. Todyshev,^{9a,9b} A. J. Lankford,¹⁰ J. W. Gary,¹¹ O. Long,¹¹ M. Franco Sevilla,¹² T. M. Hong,¹² D. Kovalskiy,¹² J. D. Richman,¹² C. A. West,¹² A. M. Eisner,¹³ W. S. Lockman,¹³ W. Panduro Vazquez,¹³ B. A. Schumm,¹³ A. Seiden,¹³ D. S. Chao,¹⁴ C. H. Cheng,¹⁴ B. Echenard,¹⁴ K. T. Flood,¹⁴ D. G. Hitlin,¹⁴ J. Kim,¹⁴ T. S. Miyashita,¹⁴ P. Ongmongkolkul,¹⁴ F. C. Porter,¹⁴ M. Röhrken,¹⁴ R. Andreassen,¹⁵ Z. Huard,¹⁵ B. T. Meadows,¹⁵ B. G. Pushpawela,¹⁵ M. D. Sokoloff,¹⁵ L. Sun,¹⁵ W. T. Ford,¹⁶ J. G. Smith,¹⁶ S. R. Wagner,¹⁶ R. Ayad,^{17,†} W. H. Toki,¹⁷ B. Spaan,¹⁸ D. Bernard,¹⁹ M. Verderi,¹⁹ S. Playfer,²⁰ D. Bettoni,^{21a} C. Bozzi,^{21a} R. Calabrese,^{21a,21b} G. Cibinetto,^{21a,21b} E. Fioravanti,^{21a,21b} I. Garzia,^{21a,21b} E. Luppi,^{21a,21b} V. Santoro,^{21a} A. Calcaterra,²² R. de Sangro,²² G. Finocchiaro,²² S. Martellotti,²² P. Patteri,²² I. M. Peruzzi,²² M. Piccolo,²² A. Zallo,²² R. Contri,^{23a,23b} M. R. Monge,^{23a,23b} S. Passaggio,^{23a} C. Patrignani,^{23a,23b} B. Bhuyan,²⁴ V. Prasad,²⁴ A. Adametz,²⁵ U. Uwer,²⁵ H. M. Lacker,²⁶ U. Mallik,²⁷ C. Chen,²⁸ J. Cochran,²⁸ S. Prell,²⁸ H. Ahmed,²⁹ A. V. Gritsan,³⁰ N. Arnaud,³¹ M. Davier,³¹ D. Derkach,³¹ G. Grosdidier,³¹ F. Le Diberder,³¹ A. M. Lutz,³¹ B. Malaescu,^{31,‡} P. Roudeau,³¹ A. Stocchi,³¹ G. Wormser,³¹ D. J. Lange,³² D. M. Wright,³² J. P. Coleman,³³ J. R. Fry,³³ E. Gabathuler,³³ D. E. Hutchcroft,³³ D. J. Payne,³³ C. Touramanis,³³ A. J. Bevan,³⁴ F. Di Lodovico,³⁴ R. Sacco,³⁴ G. Cowan,³⁵ D. N. Brown,³⁶ C. L. Davis,³⁶ A. G. Denig,³⁷ M. Fritsch,³⁷ W. Gradl,³⁷ K. Griessinger,³⁷ A. Hafner,³⁷ K. R. Schubert,³⁷ R. J. Barlow,^{38,§} G. D. Lafferty,³⁸ R. Cenci,³⁹ B. Hamilton,³⁹ A. Jawahery,³⁹ D. A. Roberts,³⁹ R. Cowan,⁴⁰ R. Cheaib,⁴¹ P. M. Patel,^{41,*} S. H. Robertson,⁴¹ B. Dey,^{42a} N. Neri,^{42a} F. Palombo,^{42a,42b} L. Cremaldi,⁴³ R. Godang,^{43,||} D. J. Summers,⁴³ M. Simard,⁴⁴ P. Taras,⁴⁴ G. De Nardo,^{45a,45b} G. Onorato,^{45a,45b} C. Sciacca,^{45a,45b} G. Raven,⁴⁶ C. P. Jessop,⁴⁷ J. M. LoSecco,⁴⁷ K. Honscheid,⁴⁸ R. Kass,⁴⁸ M. Margoni,^{49a,49b} M. Morandin,^{49a} M. Posocco,^{49a} M. Rotondo,^{49a} G. Simi,^{49a,49b} F. Simonetto,^{49a,49b} R. Stroili,^{49a,49b} S. Akar,⁵⁰ E. Ben-Haim,⁵⁰ M. Bomben,⁵⁰ G. R. Bonneaud,⁵⁰ H. Briand,⁵⁰ G. Calderini,⁵⁰ J. Chauveau,⁵⁰ Ph. Leruste,⁵⁰ G. Marchiori,⁵⁰ J. Ocariz,⁵⁰ M. Biasini,^{51a,51b} E. Manoni,^{51a} A. Rossi,^{51a} C. Angelini,^{52a,52b} G. Batignani,^{52a,52b} S. Bettarini,^{52a,52b} M. Carpinelli,^{52a,52b,¶} G. Casarosa,^{52a,52b} M. Chrzasczcz,^{52a} F. Forti,^{52a,52b} M. A. Giorgi,^{52a,52b} A. Lusiani,^{52a,52c} B. Oberhof,^{52a,52b} E. Paoloni,^{52a,52b} M. Rama,^{52a} G. Rizzo,^{52a,52b} J. J. Walsh,^{52a} D. Lopes Pegna,⁵³ J. Olsen,⁵³ A. J. S. Smith,⁵³ F. Anulli,^{54a} R. Faccini,^{54a,54b} F. Ferrarotto,^{54a} F. Ferroni,^{54a,54b} M. Gaspero,^{54a,54b} A. Pilloni,^{54a,54b} G. Piredda,^{54a} C. Bünger,⁵⁵ S. Dittrich,⁵⁵ O. Grünberg,⁵⁵ M. Hess,⁵⁵ T. Leddig,⁵⁵ C. Voß,⁵⁵ R. Waldi,⁵⁵ T. Adye,⁵⁶ E. O. Olaiya,⁵⁶ F. F. Wilson,⁵⁶ S. Emery,⁵⁷ G. Vasseur,⁵⁷ D. Aston,⁵⁸ D. J. Bard,⁵⁸ C. Cartaro,⁵⁸ M. R. Convery,⁵⁸ J. Dorfan,⁵⁸ G. P. Dubois-Felsmann,⁵⁸ W. Dunwoodie,⁵⁸ M. Ebert,⁵⁸ R. C. Field,⁵⁸ B. G. Fulsom,⁵⁸ M. T. Graham,⁵⁸ C. Hast,⁵⁸ W. R. Innes,⁵⁸ P. Kim,⁵⁸ D. W. G. S. Leith,⁵⁸ S. Luitz,⁵⁸ V. Luth,⁵⁸ D. B. MacFarlane,⁵⁸ D. R. Muller,⁵⁸ H. Neal,⁵⁸ T. Pulliam,⁵⁸ B. N. Ratcliff,⁵⁸ A. Roodman,⁵⁸ R. H. Schindler,⁵⁸ A. Snyder,⁵⁸ D. Su,⁵⁸ M. K. Sullivan,⁵⁸ J. Va'vra,⁵⁸ W. J. Wisniewski,⁵⁸ H. W. Wulsin,⁵⁸ M. V. Purohit,⁵⁹ J. R. Wilson,⁵⁹ A. Randle-Conde,⁶⁰ S. J. Sekula,⁶⁰ M. Bellis,⁶¹ P. R. Burchat,⁶¹ E. M. T. Puccio,⁶¹ M. S. Alam,⁶² J. A. Ernst,⁶² R. Gorodeisky,⁶³ N. Guttman,⁶³ D. R. Peimer,⁶³ A. Soffer,⁶³ S. M. Spanier,⁶⁴ J. L. Ritchie,⁶⁵ R. F. Schwitters,⁶⁵ J. M. Izen,⁶⁶ X. C. Lou,⁶⁶ F. Bianchi,^{67a,67b} F. De Mori,^{67a,67b} A. Filippi,^{67a} D. Gamba,^{67a,67b} L. Lanceri,^{68a,68b} L. Vitale,^{68a,68b} F. Martinez-Vidal,⁶⁹ A. Oyanguren,⁶⁹ J. Albert,⁷⁰ Sw. Banerjee,⁷⁰ A. Beaulieu,⁷⁰ F. U. Bernlochner,⁷⁰ H. H. F. Choi,⁷⁰ G. J. King,⁷⁰ R. Kowalewski,⁷⁰ M. J. Lewczuk,⁷⁰ T. Lueck,⁷⁰ I. M. Nugent,⁷⁰ J. M. Roney,⁷⁰ R. J. Sobie,⁷⁰ N. Tasneem,⁷⁰ T. J. Gershon,⁷¹ P. F. Harrison,⁷¹ T. E. Latham,⁷¹ H. R. Band,⁷² S. Dasu,⁷² Y. Pan,⁷² R. Prepost,⁷² and S. L. Wu⁷²

(BABAR Collaboration)

¹Laboratoire d'Annecy-le-Vieux de Physique des Particules (LAPP), Université de Savoie, CNRS/IN2P3, F-74941 Annecy-Le-Vieux, France

²Facultat de Física, Departament ECM, Universitat de Barcelona, E-08028 Barcelona, Spain

^{3a}INFN Sezione di Bari, I-70126 Bari, Italy

^{3b}Dipartimento di Fisica, Università di Bari, I-70126 Bari, Italy

⁴Institute of Physics, University of Bergen, N-5007 Bergen, Norway

⁵Lawrence Berkeley National Laboratory and University of California, Berkeley, California 94720, USA

⁶Institut für Experimentalphysik I, Ruhr Universität Bochum, D-44780 Bochum, Germany

- ⁷University of British Columbia, Vancouver, British Columbia V6T 1Z1, Canada
- ⁸Brunel University, Uxbridge, Middlesex UB8 3PH, United Kingdom
- ^{9a}Budker Institute of Nuclear Physics SB RAS, Novosibirsk 630090, Russia
- ^{9b}Novosibirsk State University, Novosibirsk 630090, Russia
- ^{9c}Novosibirsk State Technical University, Novosibirsk 630092, Russia
- ¹⁰University of California at Irvine, Irvine, California 92697, USA
- ¹¹University of California at Riverside, Riverside, California 92521, USA
- ¹²University of California at Santa Barbara, Santa Barbara, California 93106, USA
- ¹³Institute for Particle Physics, University of California at Santa Cruz, Santa Cruz, California 95064, USA
- ¹⁴California Institute of Technology, Pasadena, California 91125, USA
- ¹⁵University of Cincinnati, Cincinnati, Ohio 45221, USA
- ¹⁶University of Colorado, Boulder, Colorado 80309, USA
- ¹⁷Colorado State University, Fort Collins, Colorado 80523, USA
- ¹⁸Fakultät Physik, Technische Universität Dortmund, D-44221 Dortmund, Germany
- ¹⁹Laboratoire Leprince-Ringuet, Ecole Polytechnique, CNRS/IN2P3, F-91128 Palaiseau, France
- ²⁰University of Edinburgh, Edinburgh EH9 3JZ, United Kingdom
- ^{21a}INFN Sezione di Ferrara, I-44122 Ferrara, Italy
- ^{21b}Dipartimento di Fisica e Scienze della Terra, Università di Ferrara, I-44122 Ferrara, Italy
- ²²INFN Laboratori Nazionali di Frascati, I-00044 Frascati, Italy
- ^{23a}INFN Sezione di Genova, I-16146 Genova, Italy
- ^{23b}Dipartimento di Fisica, Università di Genova, I-16146 Genova, Italy
- ²⁴Indian Institute of Technology Guwahati, Guwahati, Assam 781 039, India
- ²⁵Physikalisches Institut, Universität Heidelberg, D-69120 Heidelberg, Germany
- ²⁶Institut für Physik, Humboldt-Universität zu Berlin, D-12489 Berlin, Germany
- ²⁷University of Iowa, Iowa City, Iowa 52242, USA
- ²⁸Iowa State University, Ames, Iowa 50011-3160, USA
- ²⁹Physics Department, Jazan University, Jazan 22822, Saudi Arabia
- ³⁰Johns Hopkins University, Baltimore, Maryland 21218, USA
- ³¹Laboratoire de l'Accélérateur Linéaire, IN2P3/CNRS et Université Paris-Sud 11, Centre Scientifique d'Orsay, F-91898 Orsay Cedex, France
- ³²Lawrence Livermore National Laboratory, Livermore, California 94550, USA
- ³³University of Liverpool, Liverpool L69 7ZE, United Kingdom
- ³⁴Queen Mary, University of London, London E1 4NS, United Kingdom
- ³⁵Royal Holloway and Bedford New College, University of London, Egham, Surrey TW20 0EX, United Kingdom
- ³⁶University of Louisville, Louisville, Kentucky 40292, USA
- ³⁷Institut für Kernphysik, Johannes Gutenberg-Universität Mainz, D-55099 Mainz, Germany
- ³⁸University of Manchester, Manchester M13 9PL, United Kingdom
- ³⁹University of Maryland, College Park, Maryland 20742, USA
- ⁴⁰Laboratory for Nuclear Science, Massachusetts Institute of Technology, Cambridge, Massachusetts 02139, USA
- ⁴¹McGill University, Montréal, Québec H3A 2T8, Canada
- ^{42a}INFN Sezione di Milano, I-20133 Milano, Italy
- ^{42b}Dipartimento di Fisica, Università di Milano, I-20133 Milano, Italy
- ⁴³University of Mississippi, University, Mississippi 38677, USA
- ⁴⁴Université de Montréal, Physique des Particules, Montréal, Québec H3C 3J7, Canada
- ^{45a}INFN Sezione di Napoli, I-80126 Napoli, Italy
- ^{45b}Dipartimento di Scienze Fisiche, Università di Napoli Federico II, I-80126 Napoli, Italy
- ⁴⁶NIKHEF, National Institute for Nuclear Physics and High Energy Physics, NL-1009 DB Amsterdam, Netherlands
- ⁴⁷University of Notre Dame, Notre Dame, Indiana 46556, USA
- ⁴⁸Ohio State University, Columbus, Ohio 43210, USA
- ^{49a}INFN Sezione di Padova, I-35131 Padova, Italy
- ^{49b}Dipartimento di Fisica, Università di Padova, I-35131 Padova, Italy
- ⁵⁰Laboratoire de Physique Nucléaire et de Hautes Energies, IN2P3/CNRS, Université Pierre et Marie Curie-Paris 6, Université Denis Diderot-Paris 7, F-75252 Paris, France
- ^{51a}INFN Sezione di Perugia, I-06123 Perugia, Italy
- ^{51b}Dipartimento di Fisica, Università di Perugia, I-06123 Perugia, Italy
- ^{52a}INFN Sezione di Pisa, I-56127 Pisa, Italy
- ^{52b}Dipartimento di Fisica, Università di Pisa, I-56127 Pisa, Italy
- ^{52c}Scuola Normale Superiore di Pisa, I-56127 Pisa, Italy
- ⁵³Princeton University, Princeton, New Jersey 08544, USA
- ^{54a}INFN Sezione di Roma, I-00185 Roma, Italy

- ^{54b}*Dipartimento di Fisica, Università di Roma La Sapienza, I-00185 Roma, Italy*
⁵⁵*Universität Rostock, D-18051 Rostock, Germany*
⁵⁶*Rutherford Appleton Laboratory, Chilton, Didcot, Oxon OX11 0QX, United Kingdom*
⁵⁷*CEA, Irfu, SPP, Centre de Saclay, F-91191 Gif-sur-Yvette, France*
⁵⁸*SLAC National Accelerator Laboratory, Stanford, California 94309, USA*
⁵⁹*University of South Carolina, Columbia, South Carolina 29208, USA*
⁶⁰*Southern Methodist University, Dallas, Texas 75275, USA*
⁶¹*Stanford University, Stanford, California 94305-4060, USA*
⁶²*State University of New York, Albany, New York 12222, USA*
⁶³*School of Physics and Astronomy, Tel Aviv University, Tel Aviv 69978, Israel*
⁶⁴*University of Tennessee, Knoxville, Tennessee 37996, USA*
⁶⁵*University of Texas at Austin, Austin, Texas 78712, USA*
⁶⁶*University of Texas at Dallas, Richardson, Texas 75083, USA*
^{67a}*INFN Sezione di Torino, I-10125 Torino, Italy*
^{67b}*Dipartimento di Fisica, Università di Torino, I-10125 Torino, Italy*
^{68a}*INFN Sezione di Trieste, I-34127 Trieste, Italy*
^{68b}*Dipartimento di Fisica, Università di Trieste, I-34127 Trieste, Italy*
⁶⁹*IFIC, Universitat de Valencia-CSIC, E-46071 Valencia, Spain*
⁷⁰*University of Victoria, Victoria, British Columbia V8W 3P6, Canada*
⁷¹*Department of Physics, University of Warwick, Coventry CV4 7AL, United Kingdom*
⁷²*University of Wisconsin, Madison, Wisconsin 53706, USA*

(Received 31 July 2015; published 26 January 2016)

We report on measurements of the decays of \bar{B} mesons into the semileptonic final states $\bar{B} \rightarrow D^{(*)}\pi^+\pi^-\ell^-\bar{\nu}$, where $D^{(*)}$ represents a D or D^* meson and ℓ^- is an electron or a muon. These measurements are based on 471×10^6 $B\bar{B}$ pairs recorded with the *BABAR* detector at the SLAC asymmetric B factory PEP-II. We determine the branching fraction ratios $R_{\pi^+\pi^-}^{(*)} = \mathcal{B}(\bar{B} \rightarrow D^{(*)}\pi^+\pi^-\ell^-\bar{\nu})/\mathcal{B}(\bar{B} \rightarrow D^{(*)}\ell^-\bar{\nu})$ using events in which the second B meson is fully reconstructed. We find $R_{\pi^+\pi^-} = 0.067 \pm 0.010 \pm 0.008$ and $R_{\pi^+\pi^-}^* = 0.019 \pm 0.005 \pm 0.004$, where the first uncertainty is statistical and the second is systematic. Based on these results and assuming isospin invariance, we estimate that $\bar{B} \rightarrow D^{(*)}\pi\pi\ell^-\bar{\nu}$ decays, where π denotes either a π^\pm and π^0 meson, account for up to half the difference between the measured inclusive semileptonic branching fraction to charm hadrons and the corresponding sum of previously measured exclusive branching fractions.

DOI: 10.1103/PhysRevLett.116.041801

The semileptonic decays of B mesons to final states containing a charm quark allow a measurement of the magnitude of the Cabibbo-Kobayashi-Maskawa matrix element [1,2] $|V_{cb}|$, a fundamental parameter in the standard model (SM) of particle physics that plays an important role in unitarity tests sensitive to physics beyond the SM [3]. Determinations of $|V_{cb}|$ from inclusive semileptonic decays $\bar{B} \rightarrow (X_c)\ell^-\bar{\nu}$, where the hadronic state X_c is not reconstructed, and those from the exclusive semileptonic decays $\bar{B} \rightarrow D^*\ell^-\bar{\nu}$ and $\bar{B} \rightarrow D\ell^-\bar{\nu}$, differ by nearly three standard deviations (3σ), as discussed on p. 1208 of Ref. [4]. (Throughout this Letter, whenever a decay mode is given, the charge conjugate is also implied.) The measured exclusive $\bar{B} \rightarrow X_c\ell^-\bar{\nu}$ decays, $\bar{B} \rightarrow D^{(*)}\ell^-\bar{\nu}$, $\bar{B} \rightarrow D^{(*)}\pi\ell^-\bar{\nu}$, and $\bar{B} \rightarrow D_s^{(*)+}K^-\ell^-\bar{\nu}$ [4], account for only $85 \pm 2\%$ [5] of the inclusive rate for semileptonic \bar{B} decays to charm final states. (The notation $D^{(*)}$ denotes D^0 , D^+ , D^{*0} , and D^{*+} mesons.) The decay modes measured in this Letter account for part of this difference. They also provide experimental information needed to quantify background-related systematic uncertainties in

measurements of $\bar{B} \rightarrow D^{(*)}\tau\bar{\nu}$ decays, which are sensitive to new physics contributions. A measurement [6] of these decays shows a 3.4σ deviation from the SM, and independent measurements [7,8] also exceed SM expectations.

We search for semileptonic decays of a B meson to a D or D^* meson and two additional charged pions, and we measure branching fraction ratios $R_{\pi^+\pi^-}^{(*)} = \mathcal{B}(\bar{B} \rightarrow D^{(*)}\pi^+\pi^-\ell^-\bar{\nu})/\mathcal{B}(\bar{B} \rightarrow D^{(*)}\ell^-\bar{\nu})$ relative to the topologically similar decays $\bar{B} \rightarrow D^{(*)}\ell^-\bar{\nu}$. The results are based on the complete sample of e^+e^- collision data collected at the $\Upsilon(4S)$ resonance with the *BABAR* detector at the SLAC PEP-II storage ring, corresponding to 471×10^6 $B\bar{B}$ decays (454 fb^{-1} [9]). An additional 40 fb^{-1} sample, collected at center-of-mass (c.m.) energies just below the $B\bar{B}$ threshold, is used to verify the modeling of background from $e^+e^- \rightarrow f\bar{f}(\gamma)$ continuum processes with $f = u, d, s, c, \tau$.

The *BABAR* detector, as well as the reconstruction and particle identification algorithms, are described in detail elsewhere [10]. The analysis uses Monte Carlo (MC) simulated event samples to determine efficiencies and to model backgrounds. Simulated $B\bar{B}$ decays are produced

with the EVTGEN [11] generator, with final-state radiation described using the PHOTOS [12] program. Continuum $e^+e^- \rightarrow q\bar{q}$ events are generated with the JETSET [13] program, and $e^+e^- \rightarrow \tau^+\tau^-$ events with the KK2F [14] program. The world averages quoted in Ref. [4] are used for branching fractions and form factor parameters. The GEANT4 [15] package is used to model the detector and detector response.

The intermediate process through which $D^{(*)}\pi^+\pi^-$ states arise in semileptonic B decays is unknown. We consider production via (1) three-body phase-space decays, $X_c \rightarrow D^{(*)}\pi\pi$, (2) $X_c \rightarrow D^{(*)}f_0(500)$ decays with $f_0(500) \rightarrow \pi\pi$, (3) sequential decays $X_c \rightarrow Y_c\pi$, followed by $Y_c \rightarrow D^{(*)}\pi$, and (4) $X_c \rightarrow D^{(*)}\rho$ decays with $\rho \rightarrow \pi\pi$, where X_c is one of $D_1(2420)$, $D(2S)$, or $D^*(2S)$, and Y_c is one of $D_1(2430)$, D_0^* , or D_2^* . The $D^{(*)}(2S)$ states are the first radial excitations of the ground state $D^{(*)}$ mesons and are modeled as in Ref. [5]. Our nominal signal model consists of three-body phase-space $X_c \rightarrow D^{(*)}\pi\pi$ decays with an equal mix of X_c mesons.

We reconstruct events of the type $e^+e^- \rightarrow \Upsilon(4S) \rightarrow B\bar{B}$. One of the B mesons (B_{tag}) is fully reconstructed in a hadronic final state. To reconstruct a B_{tag} candidate, a seed (one of $D^{(*)}$, $D_s^{(*)+}$, or J/ψ) is combined with up to five additional particles (pions and/or kaons), as described in Ref. [6]. The B_{tag} candidates are required to have an energy-substituted mass $m_{\text{ES}} \equiv \sqrt{s/4c^4 - |\vec{p}_{\text{tag}}/c|^2} > 5.27 \text{ GeV}/c^2$, and a difference between the beam energy and the reconstructed energy of the B_{tag} candidate $|\Delta E| \equiv |E_{\text{tag}} - \sqrt{s}/2| \leq 0.09 \text{ GeV}$, where \sqrt{s} is the total e^+e^- energy and \vec{p}_{tag} and E_{tag} are the measured B_{tag} momentum and energy in the e^+e^- c.m. frame.

For each B_{tag} candidate, we use the remaining particles in the event to search for signal \bar{B} meson candidates involving a D or D^* meson, a charged lepton, and up to two charged pions. The D^0 and D^+ candidates are reconstructed in final states involving up to four charged pions or kaons, up to one $K_S^0 \rightarrow \pi^+\pi^-$ decay, and up to one $\pi^0 \rightarrow \gamma\gamma$ decay. We require $1.845 < m(D^+) < 1.895 \text{ GeV}/c^2$ and $1.840 < m(D^0) < 1.890 \text{ GeV}/c^2$. The D^* mesons are reconstructed in $D^{*0} \rightarrow D^0\pi^0$, $D^{*0} \rightarrow D^0\gamma$, $D^{*+} \rightarrow D^0\pi^+$, and $D^{*+} \rightarrow D^+\pi^0$ decays. Electrons and muons are identified using multivariate techniques based on information from the tracking detectors, calorimeter, and muon system, and they are required to have a momentum larger than $0.6 \text{ GeV}/c$ in the c.m. frame. We reject electrons consistent with photon conversions and Dalitz decays of π^0 mesons. In cases where the flavor of the $D^{(*)}$ meson is determined by its decay products, only combinations with the correct $D^{(*)}\ell^-$ charge-flavor correlation are retained. For each $B_{\text{tag}}D^{(*)}\ell^-$ candidate we allow up to two additional charged tracks in the event, resulting in a sample consisting of $B_{\text{tag}}D^{(*)}(n\pi)\ell^-$ candidates, with ‘‘signal pion’’

multiplicity $n = 0, 1$, or 2 . Our measurement is based on the $n = 0$ and $n = 2$ samples, while the $n = 1$ sample is used to reject backgrounds in the $n = 2$ sample.

Only candidates for which all charged tracks are assigned to one or the other B meson, and where the net charge of the event is zero, are considered further. Charged B_{tag} candidates are required to have charge opposite that of the lepton candidate. We calculate E_{extra} , the energy sum of all calorimeter energy clusters with energy greater than 80 MeV that are not used in the reconstruction of the B candidates, and require $E_{\text{extra}} \leq 0.4 \text{ GeV}$. After these criteria are applied, the remaining events have, on average, about two $\Upsilon(4S) \rightarrow B_{\text{tag}}\bar{B}$ candidates per signal channel. The candidate in each $D^{(*)}(n\pi)\ell^-$ channel with the smallest $|\Delta E|$ is retained.

Each $\Upsilon(4S) \rightarrow B_{\text{tag}}\bar{B}$ candidate is fit to the hypothesized decay topology, imposing vertex and mass constraints on intermediate states in order to improve the resolution. The four-momentum of the $B_{\text{tag}}D^{(*)}(n\pi)\ell^-$ candidate is subtracted from that of the initial e^+e^- state to determine the four-momentum $p_{\text{miss}} = (E_{\text{miss}}, \vec{p}_{\text{miss}})$. For events in which a single neutrino is the only missing particle, the difference $U \equiv E_{\text{miss}} - |\vec{p}_{\text{miss}}|c$ peaks at zero with a resolution of $\approx 0.1 \text{ GeV}$; U is used to discriminate against events with additional missing particles. In contrast to the commonly used missing mass squared, which contains a factor $E_{\text{miss}} + |\vec{p}_{\text{miss}}|c \approx 2E_{\text{miss}}$, U does not depend strongly on the modeling of E_{miss} or, thus, on the decay dynamics. Hadronic B decays for which all final-state particles are reconstructed, and in which a hadron is misidentified as an electron or a muon, have $E_{\text{miss}} \approx |\vec{p}_{\text{miss}}| \approx 0$: we require $|\vec{p}_{\text{miss}}| > 0.2 \text{ GeV}/c$ to suppress these events. We impose $m(D^0\pi^\pm) - m(D^0) > 0.16 \text{ GeV}/c^2$ for the $D^0\pi^+\pi^-\ell^-\bar{\nu}$ channel to remove correctly reconstructed $B^- \rightarrow D^{*+}\pi^-\ell^-\bar{\nu}$ events with a subsequent $D^{*+} \rightarrow D^0\pi^+$ decay.

We use a separate Fisher discriminant [16] in each signal channel to further reduce the background from continuum and $B\bar{B}$ events. The variables used are E_{extra} , m_{ES} , the number of unused neutral clusters with energy greater than 80 MeV , the numbers of charged tracks and neutral clusters in the B_{tag} candidate, the second normalized Fox-Wolfram moment R_2 [17], and the c.m.-frame cosine of the angle between the thrust axes of the B_{tag} candidate and of the remaining particles in the event. The discriminants are constructed using simulated events, with the distribution of each variable reweighted to match the distribution in data. The selection requirement on the output variables is optimized assuming a branching fraction $\mathcal{B}(\bar{B} \rightarrow D^{(*)}\pi^+\pi^-\ell^-\bar{\nu}) = 0.12\%$ in each channel.

At this stage of the analysis an event may be reconstructed in more than one channel. To obtain statistically independent samples and to maximize the sensitivity to $D^{(*)}\pi^+\pi^-\ell^-\bar{\nu}$ decays, we select a unique candidate as follows. Any event found in a $D^{(*)}\ell^-\bar{\nu}$ sample is removed from all samples with one or two signal pions. If an event

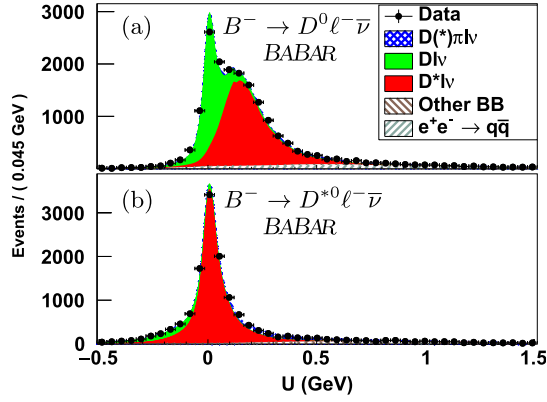


FIG. 1. Measured U distributions and results of the fit for the (a) $B^- \rightarrow D^0 \ell^- \bar{\nu}$ and (b) $B^- \rightarrow D^{*0} \ell^- \bar{\nu}$ samples.

enters two or more samples with the same number of signal pions, candidates are removed from the sample with a lower signal-to-background level. In addition, we remove from the $D^{(*)} \pi^+ \pi^- \ell^- \bar{\nu}$ samples any event found in a $D^{(*)} \pi \ell^- \bar{\nu}$ sample with $|U| < 0.1$ GeV.

The analysis procedure was developed using simulated event samples; the data for the two-pion signal modes were not examined until the selection and fit procedures were finalized. Event yields are obtained from an unbinned maximum likelihood fit to the U distribution in the range $-1.5 < U < 3.0$ GeV for each signal channel. One-dimensional probability density functions (PDFs) for the signal and background components of each sample are obtained from MC simulations using parametric kernel estimators with adaptive widths [18]. Figure 1 shows the results for the $D^{(*)0} \ell^- \bar{\nu}$ channels; the results for the $D^{(*)+} \ell^- \bar{\nu}$ channels are similar. Corresponding yields are presented in Table I.

The PDFs used in the fit to the $D^{(*)} \ell^- \bar{\nu}$ channels include the following components, whose magnitudes are parameters of the fit: $\bar{B} \rightarrow D \ell^- \bar{\nu}$, $\bar{B} \rightarrow D^* \ell^- \bar{\nu}$, $\bar{B} \rightarrow D^{(*)} \pi \ell^- \bar{\nu}$, other $B\bar{B}$ events, and continuum events. Potential contributions from $D^{(*)} \pi \pi \ell^- \bar{\nu}$ decays have a similar shape to $D^{(*)} \pi \ell^- \bar{\nu}$ decays in these channels and are included in the $\bar{B} \rightarrow D^{(*)} \pi \ell^- \bar{\nu}$ component. The PDFs used in the fit to the $D^{(*)} \pi^+ \pi^- \ell^- \bar{\nu}$ channels include the following components: $\bar{B} \rightarrow D^{(*)} \ell^- \bar{\nu}$, $\bar{B} \rightarrow D^{(*)} \pi^- \ell^- \bar{\nu}$, $\bar{B} \rightarrow D \pi^+ \pi^- \ell^- \bar{\nu}$, $\bar{B} \rightarrow D^* \pi^+ \pi^- \ell^- \bar{\nu}$, other $B\bar{B}$ events, and continuum events. Contributions to the $\bar{B} \rightarrow D^{(*)} \pi^+ \pi^- \ell^- \bar{\nu}$ channels from $\bar{B} \rightarrow D^{(*)} \pi^\pm \pi^0 \ell^- \bar{\nu}$ and $\bar{B} \rightarrow D^{(*)} \pi^0 \pi^0 \ell^- \bar{\nu}$ decays (cross feed) are treated as signal.

A fraction of signal decays are reconstructed with a B meson charge differing by ± 1 from the true B meson charge and contribute to the wrong signal channel. We determine this fraction for each signal channel in simulation and fix the corresponding yield ratio in the fit. Hadronic B meson decays in which a hadron is misidentified as a lepton can peak near $U = 0$. We estimate these small contributions using simulation and hold them fixed in the fit to the $D^{(*)} \ell^- \bar{\nu}$

TABLE I. Event yields and estimated efficiencies (ϵ) for the signal channels. The quoted uncertainties are statistical only. The fourth column gives the statistical significance, $S = \sqrt{2\Delta\mathcal{L}}$, where $\Delta\mathcal{L}$ is the difference between the log-likelihood value of the default fit and a fit with the signal yield fixed to zero. The last column gives the total significance, S_{tot} , where systematic uncertainties are included.

Channel	Yield	$\epsilon \times 10^4$	S	S_{tot}
$D^0 \ell^- \bar{\nu} \ell$	5567 ± 102	2.73 ± 0.01	> 40	> 40
$D^+ \ell^- \bar{\nu} \ell$	3236 ± 74	1.69 ± 0.01	> 40	> 40
$D^{*0} \ell^- \bar{\nu} \ell$	9987 ± 126	2.03 ± 0.01	> 40	> 40
$D^{*+} \ell^- \bar{\nu} \ell$	5404 ± 83	1.14 ± 0.01	> 40	> 40
$D^0 \pi \pi \ell^- \bar{\nu}$	171 ± 30	1.18 ± 0.03	5.4	5.0
$D^+ \pi \pi \ell^- \bar{\nu}$	56 ± 17	0.51 ± 0.02	3.5	3.0
$D^{*0} \pi \pi \ell^- \bar{\nu}$	74 ± 36	1.11 ± 0.02	1.8	1.6
$D^{*+} \pi \pi \ell^- \bar{\nu}$	65 ± 18	0.49 ± 0.02	3.3	3.0

channels. Simulation indicates that these peaking backgrounds are negligible for the $D^{(*)} \pi^+ \pi^- \ell^- \bar{\nu}$ channels.

Fits to ensembles of parametrized MC pseudoexperiments are used to validate the fit. All fitted parameters exhibit unbiased means and variances.

The results for the $D^{(*)} \pi^+ \pi^- \ell^- \bar{\nu}$ channels are shown in Fig. 2, with the corresponding signal yields in Table I. The fitted yields for all background components are consistent

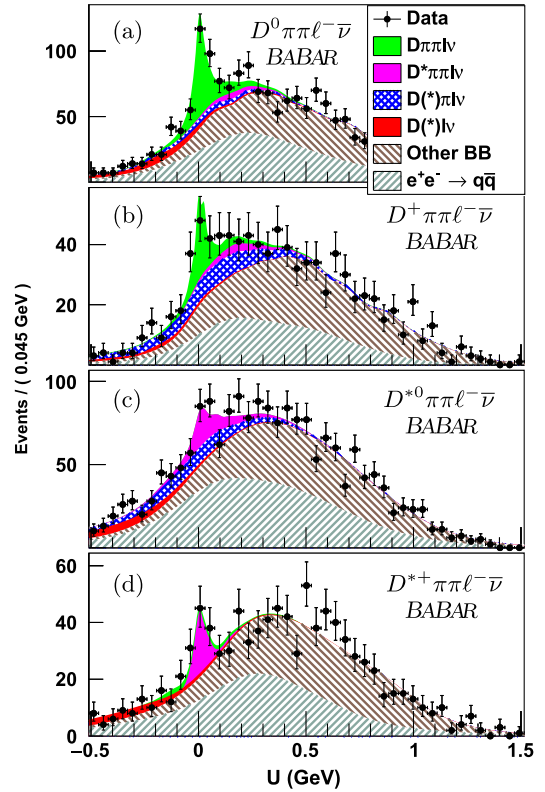


FIG. 2. Measured U distributions and results of the fit for the (a) $D^0 \pi \pi \ell^- \bar{\nu}$, (b) $D^+ \pi \pi \ell^- \bar{\nu}$, (c) $D^{*0} \pi \pi \ell^- \bar{\nu}$, and (d) $D^{*+} \pi \pi \ell^- \bar{\nu}$ samples.

with the values expected from MC simulations. The only known source of $\bar{B} \rightarrow D\pi^+\pi^-\ell^-\bar{\nu}$ decays is $\bar{B} \rightarrow D_1(2420)\ell^-\bar{\nu}$, with $D_1(2420) \rightarrow D\pi^+\pi^-$. If we remove these $D_1(2420)$ decays by vetoing events with $0.5 < m(D\pi^+\pi^-) - m(D) < 0.6 \text{ GeV}/c^2$, the signal yields are reduced to 84.3 ± 27.7 events in $D^0\pi^+\pi^-$, and 37.3 ± 15.9 in $D^+\pi^+\pi^-$, which indicates that $D_1(2420) \rightarrow D\pi^+\pi^-$ is not the only source for the observed signals.

Systematic uncertainties arising from limited knowledge of branching fractions, form factors, and detector response are evaluated. These impact the determination of the PDF shapes, fixed backgrounds, cross-feed contributions, and signal efficiencies. The leading uncertainties arise from ignorance of the potential resonance structure in the $D^{(*)}\pi^+\pi^-$ final state, the limited size of the MC samples used to derive PDFs, and the modeling of distributions of variables used in the Fisher discriminants. The dependence on the $D^{(*)}\pi\pi$ production process is investigated by using, in turn, each of the individual mechanisms listed previously to model the signal. We assign the maximum deviation between the branching fraction ratios $R_{\pi^+\pi^-}^{(*)}$ obtained from the nominal and alternative decay models as an uncertainty, giving 7.8% for $D^0\pi^+\pi^-\ell^-\bar{\nu}$, 10.5% for $D^+\pi^+\pi^-\ell^-\bar{\nu}$, 19.2% for $D^{*0}\pi^+\pi^-\ell^-\bar{\nu}$, and 13.4% for $D^{*+}\pi^+\pi^-\ell^-\bar{\nu}$. The impact of the statistical uncertainties of the PDFs are estimated from fits to 1300 simulated data sets, obtained from the primary MC samples using the bootstrapping method [19], resulting in uncertainties ranging from 6.5% ($D^0\pi^+\pi^-\ell^-\bar{\nu}$) to 21.1% ($D^{*0}\pi^+\pi^-\ell^-\bar{\nu}$). We estimate the uncertainty associated with modeling the Fisher discriminants by using the uncorrected shape of each simulated input distribution, one at a time, before imposing the selection requirement. The systematic uncertainty, given by the sum in quadrature of the differences with respect to the nominal analysis, varies from 3.7% ($D^0\pi^+\pi^-\ell^-\bar{\nu}$) to 5.2% ($D^+\pi^+\pi^-\ell^-\bar{\nu}$).

The ratios of branching fractions are calculated from the fitted yields as

$$R_{\pi^+\pi^-}^{(*)} = \frac{N_{\pi^+\pi^-}^{(*)} \epsilon_{\text{norm}}^{(*)}}{N_{\text{norm}}^{(*)} \epsilon_{\pi^+\pi^-}^{(*)}}, \quad (1)$$

where ϵ refers to the corresponding efficiency, which is calculated from MC simulations for the same type of B meson (B^- or \bar{B}^0) used in the two-pion signal ($N_{\pi^+\pi^-}^{(*)}$) and zero-pion normalization ($N_{\text{norm}}^{(*)}$) yields. The results are given in Table II. The dependence of the efficiencies on the details of the hadronic B reconstruction largely cancels in the ratio, as do some other associated systematic uncertainties and possible biases. Since semileptonic B decays proceed via a spectator diagram, the semileptonic decay widths of neutral and charged B mesons are expected to be equal. We therefore determine combined values for the B^- and \bar{B}^0 channels: these are given in Table II. Also shown are

TABLE II. Branching fraction ratios $R_{\pi^+\pi^-}^{(*)}$ for the $D^{(*)}\pi^+\pi^-\ell^-\bar{\nu}$ channels and corresponding isospin-averaged values. The first uncertainty is statistical and the second is systematic. The rightmost column gives the corresponding branching fractions, where the third uncertainty comes from the branching fraction of the normalization mode. The isospin-averaged results are quoted as B^- branching fractions.

Channel	$R_{\pi^+\pi^-}^{(*)} \times 10^3$	$\mathcal{B} \times 10^5$
$D^0\pi^+\pi^-\ell^-\bar{\nu}$	$71 \pm 13 \pm 8$	$161 \pm 30 \pm 18 \pm 8$
$D^+\pi^+\pi^-\ell^-\bar{\nu}$	$58 \pm 18 \pm 12$	$127 \pm 39 \pm 26 \pm 7$
$D^{*0}\pi^+\pi^-\ell^-\bar{\nu}$	$14 \pm 7 \pm 4$	$80 \pm 40 \pm 23 \pm 3$
$D^{*+}\pi^+\pi^-\ell^-\bar{\nu}$	$28 \pm 8 \pm 6$	$138 \pm 39 \pm 30 \pm 3$
$D\pi^+\pi^-\ell^-\bar{\nu}$	$67 \pm 10 \pm 8$	$152 \pm 23 \pm 18 \pm 7$
$D^*\pi^+\pi^-\ell^-\bar{\nu}$	$19 \pm 5 \pm 4$	$108 \pm 28 \pm 23 \pm 4$

the corresponding B^- branching fractions obtained by using Ref. [4] for the branching fractions of the normalization modes.

In conclusion, the decays $\bar{B} \rightarrow D^{(*)}(n\pi)\ell^-\bar{\nu}$ with $n = 0$ or 2 are studied in events with a fully reconstructed second B meson. We obtain the first observation of $\bar{B} \rightarrow D^0\pi^+\pi^-\ell^-\bar{\nu}$ decays and first evidence for $\bar{B} \rightarrow D^{(*)+}\pi^+\pi^-\ell^-\bar{\nu}$ decays. The branching ratios of $\bar{B} \rightarrow D^{(*)}\pi^+\pi^-\ell^-\bar{\nu}$ decays relative to the corresponding $\bar{B} \rightarrow D^{(*)}\ell^-\bar{\nu}$ decays are measured. To estimate the total $\bar{B} \rightarrow D^{(*)}\pi\pi\ell^-\bar{\nu}$ branching fraction, we use isospin symmetry and consider, in turn, each of the $\bar{B} \rightarrow X_c\ell^-\bar{\nu}$ decay models discussed above. This yields $\mathcal{B}(\bar{B} \rightarrow D^{(*)}\pi^+\pi^-\ell^-\bar{\nu})/\mathcal{B}(\bar{B} \rightarrow D^{(*)}\pi\pi\ell^-\bar{\nu}) = 0.50 \pm 0.17$, where the uncertainty is one-half of the observed spread in the values of this ratio for the different models. Applying this to the results listed in Table II gives $\mathcal{B}(\bar{B} \rightarrow D\pi\pi\ell^-\bar{\nu}) + \mathcal{B}(\bar{B} \rightarrow D^*\pi\pi\ell^-\bar{\nu}) = (0.52_{-0.07}^{+0.14+0.27})\%$, where the first uncertainty is the total experimental uncertainty and the second is due to the unknown fraction of $\bar{B} \rightarrow D^{(*)}\pi^+\pi^-\ell^-\bar{\nu}$ in $\bar{B} \rightarrow D^{(*)}\pi\pi\ell^-\bar{\nu}$ decays. These decays correspond to between one-quarter and one-half of the difference, $\Delta\mathcal{B} = (1.45 \pm 0.29)\%$ [5], between the sum of the previously measured exclusive B meson semileptonic decays to charm final states and the corresponding inclusive semileptonic branching fraction.

We are grateful for the excellent luminosity and machine conditions provided by our PEP-II colleagues, and for the substantial dedicated effort from the computing organizations that support *BABAR*. The collaborating institutions wish to thank SLAC for its support and kind hospitality. This work is supported by the DOE and the NSF (U.S.), NSERC (Canada), CEA and CNRS-IN2P3 (France), BMBF and DFG (Germany), INFN (Italy), FOM (Netherlands), NFR (Norway), MES (Russia), MINECO (Spain), STFC (United Kingdom), and BSF (U.S.-Israel). Individuals have received support from the Marie Curie EIF (European Union) and the A. P. Sloan Foundation (U.S.).

- ^{*}Deceased.
- [†]Present address: University of Tabuk, Tabuk 71491, Saudi Arabia.
- [‡]Present address: Laboratoire de Physique Nucléaire et de Hautes Energies, IN2P3/CNRS, F-75252 Paris, France.
- [§]Present address: University of Huddersfield, Huddersfield HD1 3DH, United Kingdom.
- ^{||}Present address: University of South Alabama, Mobile, Alabama 36688, USA.
- [¶]Also at Università di Sassari, I-07100 Sassari, Italy.
- [1] N. Cabibbo, *Phys. Rev. Lett.* **10**, 531 (1963).
- [2] M. Kobayashi and T. Maskawa, *Prog. Theor. Phys.* **49**, 652 (1973).
- [3] J. Charles *et al.*, *Phys. Rev. D* **91**, 073007 (2015).
- [4] K. A. Olive *et al.* (Particle Data Group), *Chin. Phys. C* **38**, 090001 (2014).
- [5] F. U. Bernlochner, Z. Ligeti, and S. Turczyk, *Phys. Rev. D* **85**, 094033 (2012).
- [6] J. P. Lees *et al.* (BABAR Collaboration), *Phys. Rev. Lett.* **109**, 101802 (2012); *Phys. Rev. D* **88**, 072012 (2013).
- [7] A. Bozek *et al.* (Belle Collaboration), *Phys. Rev. D* **82**, 072005 (2010); A. Matyja *et al.* (Belle Collaboration), *Phys. Rev. Lett.* **99**, 191807 (2007); M. Huschle *et al.* (Belle Collaboration), *Phys. Rev. D* **92**, 072014 (2015).
- [8] R. Aaij *et al.* (LHCb Collaboration), *Phys. Rev. Lett.* **115**, 111803 (2015).
- [9] J. P. Lees *et al.* (BABAR Collaboration), *Nucl. Instrum. Methods Phys. Res., Sect. A* **726**, 203 (2013).
- [10] B. Aubert *et al.* (BABAR Collaboration), *Nucl. Instrum. Methods Phys. Res., Sect. A* **479**, 1 (2002); **729**, 615 (2013).
- [11] D. J. Lange, *Nucl. Instrum. Methods Phys. Res., Sect. A* **462**, 152 (2001).
- [12] E. Barberio, B. van Eijk, and Z. Was, *Comput. Phys. Commun.* **79**, 291 (1994).
- [13] T. Sjöstrand, *Comput. Phys. Commun.* **82**, 74 (1994).
- [14] B. F. Ward, S. Jadach, and Z. Was, *Comput. Phys. Commun.* **130**, 260 (2000).
- [15] S. Agostinelli *et al.*, *Nucl. Instrum. Methods Phys. Res., Sect. A* **506**, 250 (2003).
- [16] R. A. Fisher, *Ann. Eugen.* **7**, 179 (1936).
- [17] G. C. Fox and S. Wolfram, *Nucl. Phys.* **B149**, 413 (1979); **B157**, 543(E) (1979).
- [18] K. S. Cranmer, *Comput. Phys. Commun.* **136**, 198 (2001).
- [19] I. Narsky and F. C. Porter, *Statistical Analysis Techniques in Particle Physics* (Wiley, Weinheim, 2013), Chap. 5.7.



TREASURES
@UT Dallas

School of Natural Sciences and Mathematics

Observation of $B^- \rightarrow D^ \pi^+ \pi^- \ell^- \bar{\nu}$ Decays in e^+e^- Collisions at the $\Upsilon(4s)$ Resonance*

©2016 American Physical Society

Citation:

Lees, J. P., V. Poireau, V. Tisserand, E. Grauges, et al. 2016. "Observation of $B^- \rightarrow D^{*} \pi^+ \pi^- \ell^- \bar{\nu}$ decays in e^+e^- collisions at the $\Upsilon(4S)$ resonance." Physical Review Letters 116(4), doi:10.1103/PhysRevLett.116.041801.

This document is being made freely available by the Eugene McDermott Library of The University of Texas at Dallas with permission from the copyright owner. All rights are reserved under United States copyright law unless specified otherwise.